Pergamon

Int. J. Solids Structures Vol. 34, No. 27, pp. 3619–3636, 1997

0020–7683/97 $17.00 + .00

PI: S0020–7683(96)00223–5

ANALYTICAL SOLUTION OF SPATIAL ELASTICA AND ITS APPLICATION TO KINKING PROBLEM

YASUYUKI MIYAZAKI
Department of Aerospace Engineering, College of Science and Technology, Nihon University, 7-24-1 Narashinodai, Funabashi, Chiba 274, Japan

and

KYOHEI KONDO
Department of Aeronautics, Faculty of Engineering, University of Tokyo, 7-3-1 Hongo, Bunkyo-Ku, Tokyo 113, Japan

(*Received* 17 *June* 1994; *in revised form* 20 *October* 1996)

Abstract—An analytical solution is presented for the spatially large deformation of a thin elastic rod (spatial elastica) which is naturally straight and uniform with equal principal stiffnesses and is subjected to terminal loads. The elastica can suffer not only flexure and torsion as in the classical Kirchhoff theory, but also extension and shear. The present solution is expressed in integral form and described in terms of only four parameters. This solution clears the difficulty with the polar singularity in the use of Euler angles. Hence, the numerical analysis is possible for various boundary value problems with no limitation.

In this paper we study the post-buckling behavior of an elastica under the terminal twist and uniaxial end-shortening, and give a theoretical explanation to commonly observed phenomena such as secondary bifurcation, formation of a kink, snap-through behavior. The contact problem is analyzed in the case where the elastica contacts with itself and forms a kink. These results are available for other analysis, e.g., based on finite element approximations. © 1997 Elsevier Science Ltd.

1. INTRODUCTION

The mathematical model of an elastic rod used in the analysis of geometrically nonlinear deformation in three dimensions is called spatial elastica. The analysis of the spatial elastica dates back to Kirchhoff who formulated the deformation of the spatial elastica with no axial or shear strain. Afterwards, a large amount of literature discussed the post-buckling behavior of the spatial elastica by numerical and theoretical approach [e.g., Antman (1974), Antman and Kenney (1981), Buzano *et al.* (1985)]. These obtained analytical solutions of the Kirchhoff elastica with uniformly equal principal moments of inertia of the cross-section. A few papers were concerned with the application of the solutions to boundary value problems and discussed the characteristics of the spatial deformation of an elastica [e.g. Kovari (1969), Rosenthal (1976)]. These solutions are described in integral form, and the numerical integration is needed for the analysis of the boundary value problem. However, the computation diverges at the singular point. We must therefore treat this singularity carefully in order to discuss the global behavior of the elastica.

The spatial deformation of the elastica contains various interesting aspects. Among them, unstable behaviors caused by the applied torsion is most important. When a cable is twisted with end-shortening, it makes loops under tension, and then tightens under subsequent increasing tension, i.e., kinking occurs. A rubber band forms knots only with the terminal twist and no end-shortening. It is quite difficult to analyze such phenomena because they involve a contact problem. This contact problem is therefore analyzed with quite simple mathematical models [Ross (1977), Yabta *et al.* (1982)]. In addition, the rubber knots occur with axial extension and we cannot appropriately analyze them by using the Kirchhoff theory which neglects the extension of the elastica.

In this paper, we derive an analytical solution of the equilibrium problem of the spatial deformation of an elastica formulated by Reissner (1981). The elastica has equal principal stiffnesses and can suffer flexure, torsion, extension, and shear. The external loads are applied only at the both ends of the elastica. Although this solution is expressed in terms of Euler angles, no difficulty arises in the computation. We also present the numerical procedure to analyze the self-contact problem of the elastica.

To demonstrate the validity and the applicability of the present solution, we analyze the global behavior of a uniaxially end-shortened, terminally twisted elastica. The self-contact of the elastica is also considered. There are two cases in this problem. One is the case of twisting the elastica before shortening, and the other is that of shortening it before twisting. We call the former boundary value problem "the twist-shortening problem" and the later "the shortening-twist problem". The analysis of these problems by the finite element method was difficult because the rotation of the local coordinates is very large and changes rapidly along the arc length of the elastica. But this difficulty has been recently cleared up, and such problems have been studied [Felippa and Crivelli (1991), Nour-Omid and Rankin (1991), Watanabe *et al.* (1992)]. However, since the contact problem mentioned above has not been analyzed successfully by the finite element approach yet, the results presented in this paper are available for estimating the accuracy of the results obtained by finite element approximations.

2. FORMULATION

In this study, we have four assumptions:

A1. The elastica has uniform cross-section and equal principle stiffness.
A2. Although the displacement may be large, the strains are small so that the stress resultants depend linearly on the force strains, and the stress couples depend linearly on the moment strains.
A3. There can be no deformation within the cross-section.
A4. No distributed load is applied along the elastica and only terminal loads are applied.

Let $\{\mathbf{n}_i(s,\tau)\}_{i=1,2,3}$ represent the orthogonal basis vector of a local frame attached to a typical cross-section in the deformed state, where s denotes the arc length along the line of centroid of the undeformed elastica and τ is a time parameter of the deformation process. The origin of the local frame is fixed at the centroid of the cross-section, and $\mathbf{n}_3$ remains normal to the section through the deformation process while $\mathbf{n}_1$ and $\mathbf{n}_2$ lie along the principle axes of the section. Let us introduce the reference orthogonal basis at each process denoted by $\{\mathbf{e}_i(\tau)\}_{i=1,2,3}$ and specify the orientation of the local frame by Euler angles $\{\psi(s,\tau), \theta(s,\tau), \phi(s,\tau)\}$ (Love, 1952) and the reference basis:

$$\left.\begin{aligned}
\mathbf{n}_1 &= (\cos\theta\cos\psi\cos\phi - \sin\psi\sin\phi)\mathbf{e}_1 + (\cos\theta\sin\psi\cos\phi \\
&\quad + \cos\psi\sin\phi)\mathbf{e}_2 - \sin\theta\cos\phi\mathbf{e}_3 \\
\mathbf{n}_2 &= (-\cos\theta\cos\psi\sin\phi - \sin\psi\cos\phi)\mathbf{e}_1 + (\cos\psi\cos\phi \\
&\quad - \cos\theta\sin\psi\sin\phi)\mathbf{e}_2 + \sin\theta\sin\phi\mathbf{e}_3 \\
\mathbf{n}_3 &= \sin\theta\cos\psi\mathbf{e}_1 + \sin\theta\sin\psi\mathbf{e}_2 + \cos\theta\mathbf{e}_3
\end{aligned}\right\}. \tag{1}$$

The force strains $\{\gamma_i(s,\tau)\}_{i=1,2,3}$ are defined in terms of the local basis and the position vector $\mathbf{x}$ of the centroid of the cross-section:

$$\mathbf{x}' = \gamma_1\mathbf{n}_1 + \gamma_2\mathbf{n}_2 + (1+\gamma_3)\mathbf{n}_3 \tag{2}$$

where $(\,)' = \mathrm{d}/\mathrm{d}s(\,)$. The moment strains $\{\kappa_i(s,\tau)\}_{i=1,2,3}$ are defined as follows:

$$\mathbf{n}_i' = \mathbf{k}\times\mathbf{n}_i \quad (i=1,2,3) \tag{3}$$

where

$$\mathbf{k} = \kappa_1\mathbf{n}_1 + \kappa_2\mathbf{n}_2 + \kappa_3\mathbf{n}_3. \tag{4}$$

Here γ_1 and γ_2 measure shear about the axes $\mathbf{n}_1$ and $\mathbf{n}_2$ while γ_3 measures extension. κ_1 and κ_2 measure flexure about $\mathbf{n}_1$ and $\mathbf{n}_2$ while κ_3 measures torsion. The moment strains are expressed in terms of the Euler angles introduced in eqn (1):

$$\kappa_1 = \theta'\sin\phi - \psi'\sin\theta\cos\phi, \quad \kappa_2 = \theta'\cos\phi + \psi'\sin\theta\sin\phi, \quad \kappa_3 = \phi' + \psi'\cos\theta. \tag{5}$$

Let $\{P_i(s,\tau)\}_{i=1,2,3}$ and $\{M_i(s,\tau)\}_{i=1,2,3}$ represent the components of the stress resultant and those of the stress couple about the local frame, respectively. Then, in the absence of distributed loads, the equilibrium equations with respect to these components are given as follows (Reissner, 1981):

$$\left.\begin{aligned} &P_1' - P_2\kappa_3 + P_3\kappa_2 = 0, \quad M_1' - M_2\kappa_3 + M_3\kappa_2 - P_2(1+\gamma_3) + P_3\gamma_2 = 0\\ &P_2' - P_3\kappa_1 + P_1\kappa_3 = 0, \quad M_2' - M_3\kappa_1 + M_1\kappa_3 - P_3\gamma_1 + P_1(1+\gamma_3) = 0\\ &P_3' - P_1\kappa_2 + P_2\kappa_1 = 0, \quad M_3' - M_1\kappa_2 + M_2\kappa_1 - P_1\gamma_2 + P_2\gamma_1 = 0 \end{aligned}\right\}. \tag{6}$$

According to the assumptions A1 and A2, the constitutive relations are expressed as follows [Iura and Atruli (1988), Goto *et al.* (1990)]:

$$P_1 = K\gamma_1, \quad P_2 = K\gamma_2, \quad P_3 = K_3\gamma_3, \quad M_1 = A\kappa_1, \quad M_2 = A\kappa_2, \quad M_3 = A_3\kappa_3 \tag{7}$$

where A, A_3, K, K_3 are flexural, torsional, shear, and extensional rigidity, respectively. They are assumed to be constant along the arc length.

Let us nondimensionalize length and coordinates by the lastica length l, the moment strains by π/l, the stress resultants by the Euler Buckling load $A\pi^2/l^2$, the stress couples by $A\pi/l$, and express the nondimensionalized values by the same characters hereinafter. Furthermore, let us introduce non-dimensional stiffness ratios p, q, a as follows:

$$p = \frac{A\pi^2}{l^2K}, \quad q = \frac{A\pi^2}{l^2K_3}, \quad a = \frac{A}{A_3}. \tag{8}$$

p, q, and a represent the stiffness ratios of flexure to shear, extension, and torsion, respectively. Then, by using eqn (7), we can integrate the equilibrium eqn (6) into

$$(P_1, P_2, P_3) = R(-\sin\theta\cos\phi, \sin\theta\sin\phi, \cos\theta) \tag{9}$$

$$\left.\begin{aligned} &\kappa_1P_1 + \kappa_2P_2 + \frac{\kappa_3}{a}P_3 = \text{const} \equiv RC_o\\ &\kappa_1^2 + \kappa_2^2 + 2P_3 + (q-p)P_3^2 = \text{const} \equiv C_1\\ &\kappa_3 = \text{const} \equiv \kappa_3^0 \end{aligned}\right\} \tag{10}$$

where $\{R(\tau), C_0(\tau), \mathrm{C}_1(\tau), \kappa_3^o(\tau)\}$ are integral constants. R represents the amount of the applied terminal force. Equation (9) is obtained by taking the direction of $\mathbf{e}_3$ opposite to that of the terminal force. Therefore the orientation of the reference frame should be

specified by two Euler angles which we denote $\{\psi_p(\tau), \theta_p(\tau)\}$:

$$\left.\begin{aligned} \mathbf{e}_1 &= \cos\theta_p \cos\psi_p \mathbf{E}_1 + \cos\theta_p \sin\psi_p \mathbf{E}_2 - \sin\theta_p \mathbf{E}_3 \\ \mathbf{e}_2 &= -\sin\psi_p \mathbf{E}_1 + \cos\psi_p \mathbf{E}_2 \\ \mathbf{e}_3 &= \sin\theta_p \cos\psi_p \mathbf{E}_1 + \sin\theta_p \sin\psi_p \mathbf{E}_2 + \cos\theta_p \mathbf{E}_3 \end{aligned}\right\}. \tag{11}$$

Substituting eqns (5), (7), and (9) into eqn (10) gives the differential expression of (s, ψ, ϕ) with respect to θ,

$$\left.\begin{aligned} \frac{\mathrm{d}s}{\mathrm{d}\theta} &= f(\theta), \quad \frac{\mathrm{d}\psi}{\mathrm{d}\theta} = \frac{(aC_0 - \kappa_3^o \cos\theta)}{a\sin^2\theta} f(\theta) \\ \frac{\mathrm{d}\phi}{\mathrm{d}\theta} &= \frac{(a\sin^2\theta + \cos^2\theta)\kappa_3^o - aC_0\cos\theta}{a\sin^2\theta} f(\theta) \end{aligned}\right\} \tag{12}$$

where

$$\left.\begin{aligned} f(\theta) &= \pm \frac{\sin\theta}{\sqrt{g(\cos\theta)}} \\ g(w) &= \{2C_1 - 2Rw + (p-q)R^2 w^2\}(1-w^2) - \left(C_0 - \frac{\kappa_3^o}{a} w\right)^2 \end{aligned}\right\}. \tag{13}$$

The differential expression of the components $\{x(s,\tau), y(s,\tau), z(s,\tau)\}$ of the position vector $\mathbf{x}$ is obtained from the substitution of eqns (1), (7), (9) and (12) into eqn (2):

$$\left.\begin{aligned} \mathbf{x} &= x\mathbf{e}_1 + y\mathbf{e}_2 + z\mathbf{e}_3, & \frac{\mathrm{d}x}{\mathrm{d}\theta} &= f(\theta)\{1 + (q-p)R\cos\theta\}\sin\theta\cos\psi \\ \frac{\mathrm{d}y}{\mathrm{d}\theta} &= f(\theta)\{1 + (q-p)R\cos\theta\}\sin\theta\sin\psi, & \frac{\mathrm{d}z}{\mathrm{d}\theta} &= f(\theta)[\{1 + (q-p)R\cos\theta\}\cos\theta + pR] \end{aligned}\right\}. \tag{14}$$

From a detailed calculation, we discover that two of the solutions of the equation $g(w) = 0$ satisfy $-1 \leqslant w \leqslant 1$, and one of other solutions satisfies $|w| \geqslant 1$. Therefore $g(w)$ can be expressed as follows:

$$g(w) = (\cos 2\theta_m - w)(w - \cos 2\theta_n)(1 + \cos 2\varphi w)(\mu_1 + \mu_2 w) \tag{15}$$

By comparing eqn (13) with (15), we can express the integral constants $\{R(\tau), C_0(\tau), C_1(\tau), \kappa_3^o(\tau)\}$ and the parameters $\{\mu_1, \mu_2\}$ in terms of stiffness ratios and four parameters $\{\theta_m(\tau), \theta_n(\tau), \varphi(\tau), \eta(\tau)\}$ as follows:

$$\left.\begin{aligned} R &= -\eta^2 \cos 2\varphi, \quad \kappa_3^o = a(\rho - \lambda), \quad C_0 = \rho + \lambda \\ C_1 &= C_0^2 + \mu_1 \cos\theta_m \cos\theta_n \\ \mu_1 &= \eta^2[2 + (q-p)\eta^2\{\cos 2\varphi(\cos 2\theta_m + \cos 2\theta_n) - 1\}], \quad \mu_2 = (q-p)\eta^4 \cos 2\varphi \end{aligned}\right\} \tag{16}$$

where

$$\rho = \sqrt{2(\mu_1 - \mu_2)}\cos\theta_m \cos\theta_n \sin\varphi, \quad \lambda = \sqrt{2(\mu_1 + \mu_2)}\sin\theta_m \sin\theta_n \cos\varphi. \tag{17}$$

Let us introduce new parameter t, and functions $C_g(t)$, $S_g(t)$ as

$$\left.\begin{aligned} C_g(t) &\equiv \frac{\cos 2\theta_m + \cos 2\theta_n}{2} + \frac{\cos 2\theta_m - \cos 2\theta_n}{2}\cos t = \cos\theta \\ S_g(t) &\equiv \sqrt{1 - C_g(t)^2} = \sin\theta \end{aligned}\right\}. \tag{18}$$

Then, from eqns (10)–(13), an analytical solution is described in terms of ten parameters $\{\theta_m(\tau), \theta_n(\tau), \varphi(\tau), \eta(\tau), t_o(\tau), t_e(\tau), \psi_o(\tau), \phi_o(\tau), \psi_p(\tau), \theta_p(\tau)\}$ and the integral variable t $[t_o \leqslant t \leqslant t_e]$ as follows:

$$\left.\begin{aligned} s &= s(t) = \int_{t_o}^{t} F(t)\,\mathrm{d}t \\ \theta &= \theta(t) = \cos^{-1}[C_g(t)] \\ \psi &= \psi(t) = \psi_o + \Omega(t) + \Gamma(t) \\ \phi &= \phi(t) = \phi_o + \Omega(t) - \Gamma(t) + \pi(a-1)(\rho - \lambda)s(t) \\ \mathbf{x} &= \mathbf{x}(t) = x\mathbf{e}_1(\theta_p, \psi_p) + y\mathbf{e}_2(\theta_p, \psi_p) + z\mathbf{e}_3(\theta_p, \psi_p) \\ x &= x(t) = \int_{t_o}^{t} F(t)\{1 - (q-p)\eta^2 \cos 2\varphi C_g(t)\}S_g(t)\cos\psi(t)\,\mathrm{d}t \\ y &= y(t) = \int_{t_o}^{t} F(t)\{1 - (q-p)\eta^2 \cos 2\varphi C_g(t)\}S_g(t)\sin\psi(t)\,\mathrm{d}t \\ z &= z(t) = \int_{t_o}^{t} F(t)[\{1 - (q-p)\eta^2 \cos 2\varphi C_g(t)\}C_g(t) - p\eta^2\cos 2\varphi]\,\mathrm{d}t \end{aligned}\right\} \tag{19}$$

where

$$\left.\begin{aligned} F(t) &= \frac{1}{\sqrt{[1 + \cos 2\varphi C_g(t)][\mu_1 + \mu_2 C_g(t)]}} \\ \Omega(t) &= \int_{t_o}^{t} F(t)\frac{\rho}{1 + C_g(t)}\,\mathrm{d}t, \quad \Gamma(t) = \int_{t_o}^{t} F(t)\frac{\lambda}{1 - C_g(t)}\,\mathrm{d}t \end{aligned}\right\} \tag{20}$$

t_o and t_e are the values of t at $s = 0$ and $s = l$, respectively. The integral variable t monotonically increases as s increases, and therefore we call it generalized arc-length hereinafter. The elastica curve is determined only by four parameters $(\theta_m, \theta_n, \varphi, \eta)$. Other parameters $(t_o, t_e, \psi_o, \phi_o, \psi_p, \theta_p)$ give no principal effect on the curve. This solution is reduced to that of the Kirchhoff equations by setting $p = q = 0$.

3. POLAR SINGULARITY ASSOCIATED WITH EULER ANGLES

In the present solution (19), the effect of the polar singularity associated with Euler angles appears seriously in the functions $\Omega(t)$ and $\Gamma(t)$. In eqn (20), $C_g(\pi) = -1$ and $\rho = 0$ hold if $\theta_n = \pi/2$, and $C_g(0) = 1$ and $\lambda = 0$ hold if $\theta_m = 0$. Hence, in each case, the values of $\Omega(t)$ or $\Gamma(t)$ cannot be computed from eqn (20). After integrating $\Omega(t)$ by parts, we obtain

$$\begin{aligned} \Omega(t) = &-\left[\frac{\cot(t/2)}{|\cot(t/2)|}\sin^{-1}\left(\frac{c_{mn}}{\sqrt{c_{mn}^2 + \cot^2(t/2)}}\right)\sqrt{2(\mu_1 - \mu_2)}\sin\varphi F(t)\right]_{t_o}^{t} \\ &+ \int_{t_o}^{t}\frac{\cot(t/2)}{|\cot(t/2)|}\sin^{-1}\left(\frac{c_{mn}}{\sqrt{c_{mn}^2 + \cot^2(t/2)}}\right)\sqrt{2(\mu_1 - \mu_2)}\sin\varphi\frac{\mathrm{d}F(t)}{\mathrm{d}t}\,\mathrm{d}t \end{aligned} \tag{21}$$

where $c_{mn} = \cos\theta_n/\cos\theta_m$. In the case $\theta_n = \pi/2$, c_{mn} vanishes and $\Omega(t)$ remains invariant for $t \neq \pi$ as in eqn (21). At $t = \pi$,

$$\left|\frac{\cot(t/2)}{|\cot(t/2)|}\sin^{-1}\left(\frac{c_{mn}}{\sqrt{c_{mn}^2+\cot^2(t/2)}}\right)\sqrt{2(\mu_1-\mu_2)}\sin\varphi F(t)\right| = \frac{\pi}{2} \tag{22}$$

and $\Omega(t)$ changes its value stepwise by the amount $\pi/2$. This means that the function $\rho/[1+C_g(t)]$ in eqn (20) acts as a delta function. A similar result holds for $\Gamma(t)$. The value of $\sin\theta_m/\sin\theta_n$ $[\equiv s_{mn}]$ holds the key to the behavior of $\Gamma(t)$ instead of c_{mn}. Thus ψ and ϕ also changes stepwisely at the singular points. If we use eqn (21) for the calculation of $\Omega(t)$, no numerical difficulty arises.

It must be mentioned that we cannot uniquely determine the value of c_{mn} or s_{mn} when $\theta_m = \theta_n = 0$ or $\pi/2$. The buckling point of a rod subjected to terminal twist and uniaxial compression is under this condition. However, we can determine them theoretically by using the relation of the buckling load and the twist angle obtained from the linear analysis [Zachmann (1979)]. Thus there remains no difficulty in computing any boundary value problem. Note that we can never predict this special behavior of ψ, ϕ at the singular points by means of numerical integration of eqns (5) and (6), e.g., using Runge-Kutta or finite difference procedure [Huddleston (1978), Nordgren (1974)].

4. CONTACT PROBLEM

We assume the contact condition when the elastica contacts with itself as follows:

1. No distortion is caused within the cross-section by the contact force.
2. The cross-section is a circle of radius d and the elastica contacts at one point on its surface.
3. The contact force acts towards the centroid of the cross-section containing the contact point.

When the elastica contacts with itself, it can be divided into three elements as in Fig. 1. The first element is the part from the origin of the elastica to the contact point. The second element is the loop formed by the contact point. The third element is the part from the contact point to the end of the elastica. As mentioned in Section 2, the z-axis of the reference frame is parallel to the direction of the external force applied to the end of the element. Thereby the reference basis of the second element (loop element) does not coincide with those of other elements while the first and third elements have the same reference basis.

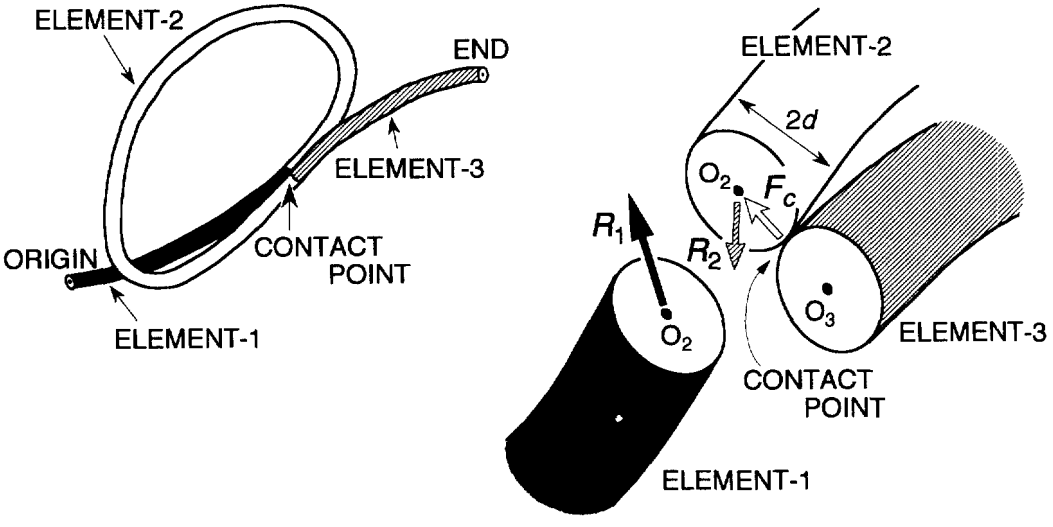

Fig. 1. Contact problem.

The relation of the reference frame $\{\mathbf{e}_i^{[2]}(\tau)\}_{i=1,2,3}$ of the second loop and the frame $\{\mathbf{e}_i(\tau)\}_{i=1,2,3}$ of other elements can be described by two rotation angles $\{\psi_c(\tau), \theta_c(\tau)\}$:

$$\left.\begin{aligned}\mathbf{e}_1^{[2]} &= \cos\theta_c\cos\psi_c\mathbf{e}_1 + \cos\theta_c\sin\psi_c\mathbf{e}_2 - \sin\theta_c\mathbf{e}_3\\ \mathbf{e}_2^{[2]} &= -\sin\psi_c\mathbf{e}_1 + \cos\psi_c\mathbf{e}_2\\ \mathbf{e}_3^{[2]} &= \sin\theta_c\cos\psi_c\mathbf{e}_1 + \sin\theta_c\sin\psi_c\mathbf{e}_2 + \cos\theta_c\mathbf{e}_3\end{aligned}\right\}. \tag{23}$$

The contact conditions at the origin of the second element are given as follows:

$$\left.\begin{aligned}&\{M_1(t_e), M_2(t_e), M_3(t_e)\}^{[1]} = \{M_1(t_o), M_2(t_o), M_3(t_o)\}^{[2]}\\ &\{\mathbf{n}_1(t_e), \mathbf{n}_2(t_e), \mathbf{n}_3(t_e)\}^{[1]} = \{\mathbf{n}_1(t_o), \mathbf{n}_2(t_o), \mathbf{n}_3(t_o)\}^{[2]}\\ &-R^{[2]}\mathbf{e}_3^{[2]} + R^{[1]}\mathbf{e}_3 = F_c\mathbf{E}_c\end{aligned}\right\} \tag{24}$$

where F_c is the amount of the contact force, and $\mathbf{E}_c$ is a unit vector in the direction of the contact force and described as

$$\mathbf{E}_c = \cos\omega_c\mathbf{n}_1(t_o)^{[2]} + \sin\omega_c\mathbf{n}_2(t_o)^{[2]}. \tag{25}$$

The contact conditions at the end of the second element are given as follows:

$$\left.\begin{aligned}&\{M_1(t_e), M_2(t_e), M_3(t_e)\}^{[2]} = \{M_1(t_o), M_2(t_o), M_3(t_o)\}^{[3]}\\ &\{\mathbf{n}_1(t_e), \mathbf{n}_2(t_e), \mathbf{n}_3(t_e)\}^{[2]} = \{\mathbf{n}_1(t_o), \mathbf{n}_2(t_o), \mathbf{n}_3(t_o)\}^{[3]}\\ &\mathbf{x}(t_e)^{[2]} = -2d\mathbf{E}_c, \quad \mathbf{E}_c\cdot\mathbf{n}_3(t_e)^{[2]} = 0, \quad R^{[2]} = R^{[3]}\end{aligned}\right\}. \tag{26}$$

The number of the unknowns is thirty:

$$(\psi_p, \theta_p), \quad (\omega_c, F_c, \psi_c, \theta_c), \quad \{\theta_m, \theta_n, \varphi, \eta, t_o, t_e, \psi_c, \phi_o\}^{[N]} \quad (N = 1, 2, 3).$$

The contact conditions which these unknowns must satisfy are eqns (24) and (26). The number of these conditions is twenty. Therefore the boundary value problem can be solved if ten conditions are given at the origin or the end of the elastica. The above unknowns are called "the system parameters" in the following. Note that the determination of the values of generalized arc-length $\{t_o, t_e\}^{[N]}$ corresponds to the search of the contact point.

5. "THE TWIST-SHORTENING PROBLEM"

In this section, we study in detail "the twist-shortening problem" proposed in the Introduction. In Fig. 2, one end of the straight elastica is clamped. The other end is previously twisted through the angle of ϕ_m about the axis joining the both ends, and later subjected to the end-shortening of the amount ξl about this axis ($\xi < 1$). No displacement or rotation is allowed in any direction out of this axis. The problem is governed by six parameters $(a, p, q, d/l, \phi_m, \xi)$. Let us locate the fixed spatial basis $\{\mathbf{E}_i\}_{i=1,2,3}$ such that

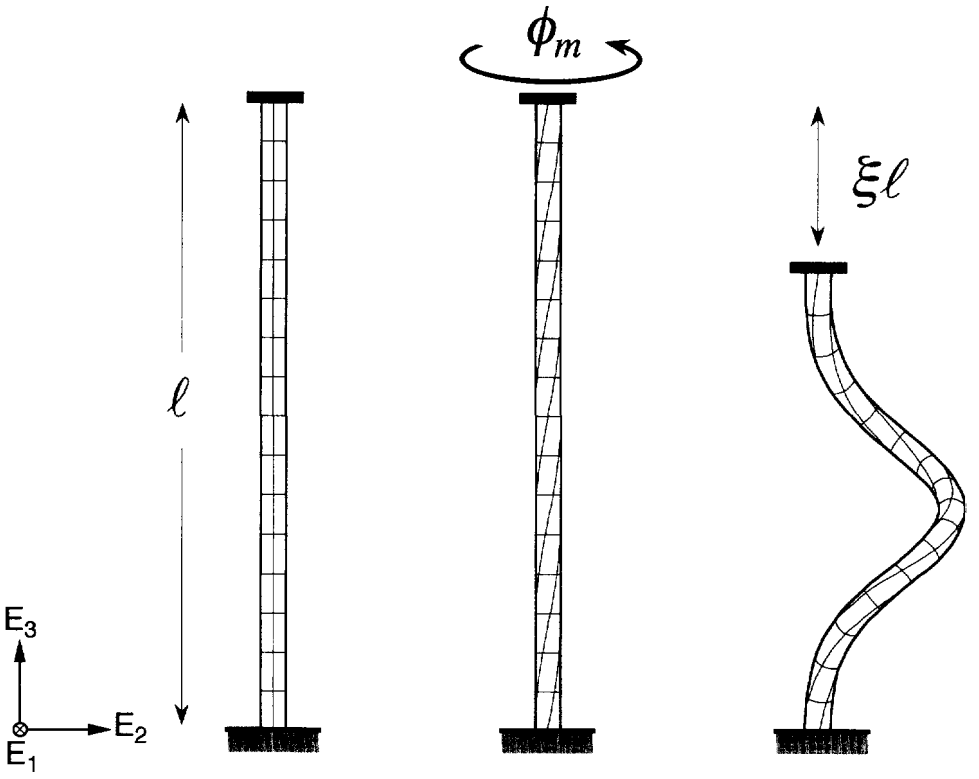

Fig. 2. Twist-shortening problem.

$\mathbf{E}_i = \mathbf{n}_i(t_o)$. Then the boundary conditions are written as follows:

$$\left.\begin{aligned} &\mathbf{n}_i(t_o) = \mathbf{E}_i, \quad s(t_e) = 1, \quad \mathbf{x}(t_e) = (1-\xi)\mathbf{E}_3 \\ &\{\mathbf{n}_1(t_e), \mathbf{n}_2(t_e), \mathbf{n}_3(t_e)\} = \{\mathbf{E}_1, \mathbf{E}_2, \mathbf{E}_3\}\begin{bmatrix} \cos\phi_m & -\sin\phi_m & 0 \\ \sin\phi_m & \cos\phi_m & 0 \\ 0 & 0 & 1 \end{bmatrix} \end{aligned}\right\}. \tag{27}$$

The twist-shortening problem is solvable under these ten independent conditions as mentioned at the end of the previous section. Taking into account the symmetry of the deformation, we obtain

$$\psi_o = \phi_o = 0, \quad \psi_p = 0, \quad \theta_p = -\cos^{-1}[C_g(t_o)], \quad t_e = 2(k+1)\pi - t_o \tag{28}$$

where k is a positive integer and represents the degree of the buckling mode. Thus the number of the unknown system parameters reduces by five. The independent boundary conditions are also reduced from ten to five:

$$\left.\begin{aligned} &s(t_e) = 1, \quad x(t_e) = (1-\xi)S_g(t_o), \quad z(t_e) = (1-\xi)C_g(t_o) \\ &\psi(t_e) = 2i\pi, \quad \phi(t_e) = \phi_m - 2i\pi \end{aligned}\right\} \tag{29}$$

where i is an integer.

5.1. *The stiffness ratio a and the twist angle ϕ_m*

Consider the case where there is no contact point. The solution and the boundary conditions are given by eqns (19) and (29), respectively. The stiffness ratio a explicitly relates only to the Euler angle ϕ (see eqn (19)). The terminal-twist angle ϕ_m also relates only to ϕ as in eqn (29). Therefore the system parameters which describe the boundary

value problem represented by (a, p, q, ϕ_m, ξ) satisfy the boundary conditions represented by $(\tilde{a}, p, q, \tilde{\phi}_m, \xi)$ if the following relation holds:

$$\begin{aligned}\tilde{\phi}_m &= \phi_m + \pi(\tilde{a}-a)(\rho-\lambda)s(t_e) \\ &= \phi_m + \pi\left(\frac{\tilde{a}}{a}-1\right)\kappa_3^o. \end{aligned} \tag{30}$$

This result implies that we can obtain the solutions for arbitrary values of the stiffness ratio $\tilde{a}$ by using the solution for a given stiffness ratio a. This feature of the solution is quite important and convenient in the estimation of the influence of the stiffness ratio a on the solution. Note that the deformation in the absence of torsion is identical for the elastica of arbitrary stiffness ratio a. The same relation holds in the contact problem because the torsion is identical for all elements.

5.2. *Kirchhoff model*

If $p = q = 0$, the elastica is inextensible and its cross-section is perpendicular to the line of the centroid after the deformation, i.e., the elastica obeys the Kirchhoff hypothesis. In this subsection, we study the spatial behavior of a Kirchhoff elastica under the twist-shortening by using eqn (19). The integrals in eqn (19) are performed numerically with Gaussian integral procedure. Therefore the numerical values shown in the following involve very small numerical errors.

5.2.1. *Unstable behavior of spatial elastica.* Figure 3 shows the deformed shapes of the elastica under the axial end-shortening with no terminal twist, i.e., $\phi_m = 0$. The stiffness ratio is $a = 1$, and the radius of the cross-section is $d = 0.02\ l$. The elastica buckles at $\xi = 0$, and buckles out of plane at $\xi = 0.667$. It deforms spatially for the subsequent end-shortening, and contacts with itself at $\xi = 0.811$. The strain energy stored in the spatially deformed elastica is smaller than that in the planar elastica for $\xi > 0.667$. Therefore the elastica deforms spatially for $\xi > 0.667$. You can really watch such a secondary buckling phenomenon when you compress a string uniaxially. The bifurcation point of this secondary buckling is determined according to the value of the stiffness ratio a. We can analyze this bifurcation by using the perturbation method as follows: when the elastica deforms in plane under $\phi_m = 0$, the system parameters are $(\theta_m, t_o, \varphi) = (0, 0, 0)$, and θ_n is determined

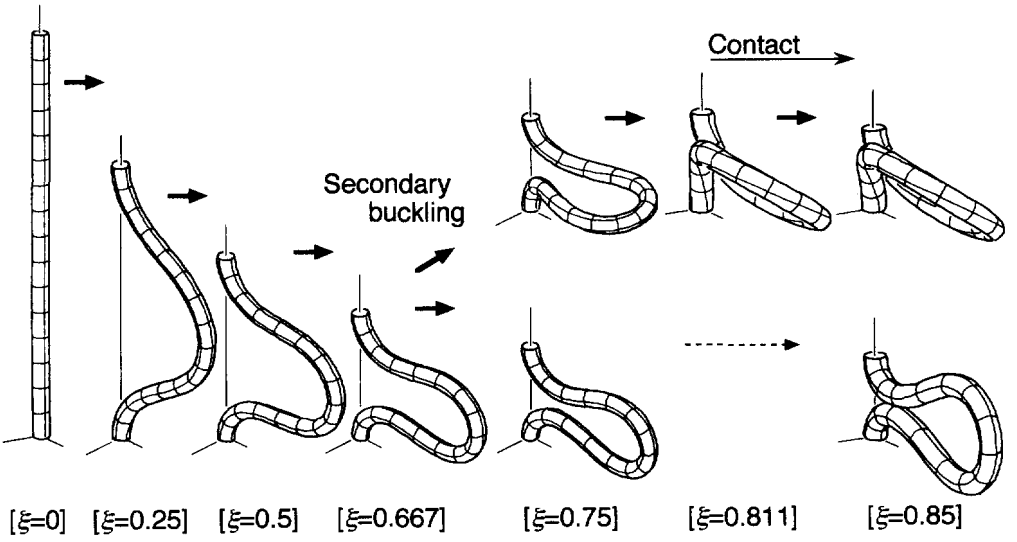

Fig. 3. Deformed shapes ($\phi_m = 0$).

by the following equations.

$$\xi = 1-\left[\int_0^{\pi} \frac{C_g(t)}{\sqrt{1+C_g(t)}}\mathrm{d}t \Big/ \int_0^{\pi} \frac{\mathrm{d}t}{\sqrt{1+C_g(t)}}\right], \quad C_g(t) = \frac{1+\cos 2\theta_n}{2} + \frac{1-\cos 2\theta_n}{2}\cos t. \tag{31}$$

These results are obtained from eqns (19), (20), and (29). Now we consider the small perturbation of the twist angle $\varepsilon\phi_m^*$, and that of the shortening ratio $\varepsilon\xi^*$ from $(\phi_m, \xi) = (0, \xi_o)$, and denote the resulting perturbation of other variables as $\varepsilon(\,)^*$ where $\varepsilon \ll 1$

$$\phi_m = \varepsilon\phi_m^*, \quad \xi = \xi_o + \varepsilon\xi^*, \quad (\,) = (\,) + \varepsilon(\,)^*. \tag{32}$$

After a few calculations by using eqns (19), (20), and (29), the relations between the perturbations of the system parameters $(\theta_m^*, \theta_n^*, \varphi^*, \eta^*, t_o^*)$ and (ϕ_m^*, ξ^*) are obtained as follows:

$$\left.\begin{aligned} &J_o\theta_m^* = -\frac{J_\varphi}{\sqrt{2}}\phi_m^*, \quad J_o\varphi^* = \frac{J_m}{4\sqrt{2}\cos\theta_n}\phi_m^* \\ &t_o^* = 0, \quad \left[\int_0^{\pi} \frac{\{1+\xi_o+C_g(t)\}(1-\cos t)}{[\sqrt{1+C_g(t)}]^3}\mathrm{d}t\right]\theta_n^* = \frac{2J_s}{\sin 2\theta_n}\xi^* \end{aligned}\right\} \tag{33}$$

where

$$\left.\begin{aligned} &J_o = 2J_mJ_\varphi + (a-1)[J_m - 2\sin\theta_n J_\varphi]J_s, \quad J_m = \sin\theta_n \int_0^{\pi} \frac{(1+\cos t)}{[\sqrt{1+C_g(t)}]^3}\mathrm{d}t - \frac{J_z}{\sin\theta_n} \\ &J_z = \int_0^{\pi} \frac{C_g(t)}{\sqrt{1+C_g(t)}}\mathrm{d}t, \quad J_s = \int_0^{\pi} \frac{1}{\sqrt{1+C_g(t)}}\mathrm{d}t, \quad J_\varphi = \int_0^{\pi} \frac{1}{[\sqrt{1+C_g(t)}]^3}\mathrm{d}t \end{aligned}\right\}. \tag{34}$$

Let ϕ_m^* and ξ^* lead to 0. Then eqn (33) must have non-trivial solution of $(\theta_m^*, \theta_n^*, \varphi^*, \eta^*, t_o^*)$ at the bifurcation point. Thus, $J_o = 0$ must hold there. Accordingly we can determine the value of θ_n for a given end-shortening ξ_o by eqn (31) and the value of the stiffness ratio a for which the bifurcation occurs at ξ_o by:

$$a = 1 - \frac{2J_mJ_\varphi}{J_s[J_m + 2J_\varphi\sin\theta_n]}. \tag{35}$$

Figure 4 plots the bifurcation point ξ_o as a function of a. This secondary buckling is caused by the transition of the energy from the bending mode to the torsional mode. So the bifurcation occurs with smaller end-shortening for larger flexural rigidity as in Fig. 4. Figure 4 also shows that the bifurcation never occurs for $a < 0.5$ or $\xi < 0.371$. At $\xi = 0.371$, the resulting perturbation of the torsion $(\kappa_3)^*$ vanishes, and this point is the bifurcation point in the case the applied torsion is prescribed to 0. Kovari (1969) treated this problem.

Figure 5 shows the deformed shapes of the elastica in the end-shortening process under $\phi_m = 2\pi$. The contact of the elastica is not taken into account. The elastica buckles spatially at $\xi = 0$. It forms a planar loop at $\xi = 0.667$, and deforms in plane for further end-shortening. If the contact model is used in the calculation, the elastica contacts with itself at $\xi = 0.660$ and deforms with the contact for further end-shortening. The planar loop solution exists also in $0 < \xi < 0.667$, i.e., the point $\xi = 0.667$ is the bifurcation point from the spatial into the planar solution. We call the former the non-kinking solution and the

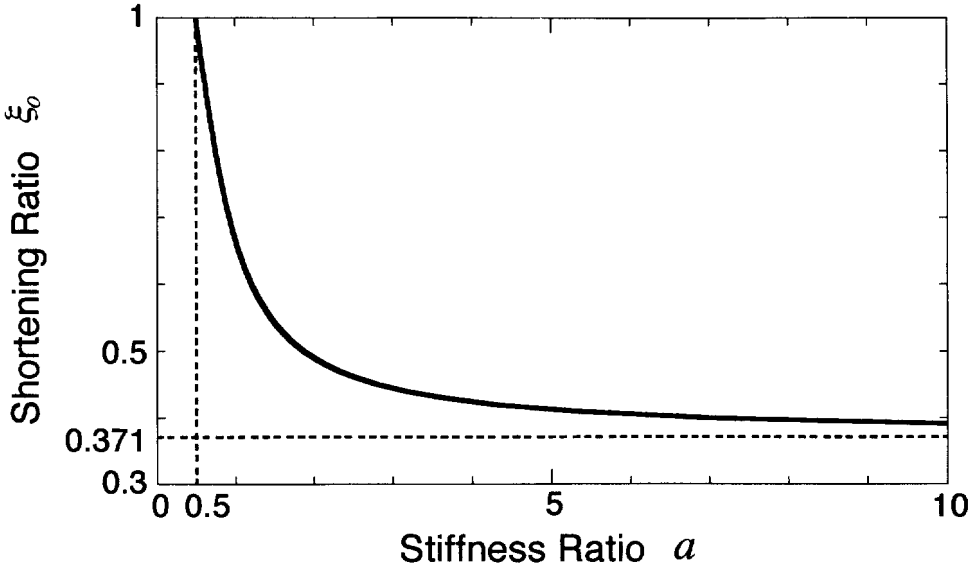

Fig. 4. Secondary buckling point ($\phi_m = 0$).

later the semi-kinking solution. This bifurcation point is analyzed in the same manner as the previous case $\phi_m = 0$. For the semi-kinking solution, the system parameters are $(\theta_m, \theta_n, t_o) = (0, \pi/2, \pi)$, and φ is determined by the following equation.

$$\xi = 1 - I_z/I_s \tag{36}$$

where

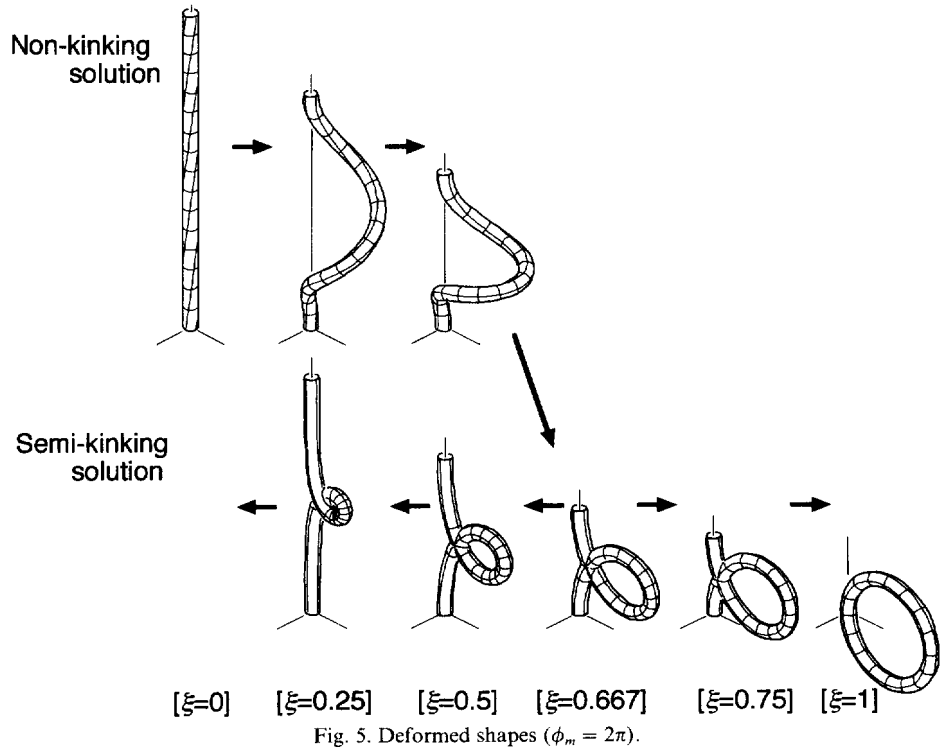

Fig. 5. Deformed shapes ($\phi_m = 2\pi$).

$$I_s = \int_0^{\pi} \frac{1}{\sqrt{1+\cos 2\varphi \cos t}}\,dt, \quad I_z = \int_0^{\pi} \frac{\cos t}{\sqrt{1+\cos 2\varphi \cos t}}\,dt. \tag{37}$$

The perturbation of each parameter relates to others as follows:

$$\left.\begin{aligned} I_o\theta_m^* &= \frac{-I_n \cos\varphi}{2\sqrt{2}}\phi_m^*, \quad I_o\theta_n^* = \frac{I_m}{8\sqrt{2}}\phi_m^* \\ t_o^* &= -\frac{\sqrt{2}I_z \cos\theta_n \cos 2\varphi}{|\sin\varphi|}\theta_m^*, \quad \left[\sin 2\varphi \int_0^{\pi} \frac{(1-\xi)\cos t - \cos^2 t}{(\sqrt{1+\cos 2\varphi \cos t})^3}\,dt\right]\varphi^* = -I_s\xi^* \end{aligned}\right\} \tag{38}$$

where

$$\left.\begin{aligned} I_m &= \int_0^{\pi} \frac{1+\cos t}{[\sqrt{1+\cos 2\varphi \cos t}]^3}\,dt, \quad I_n = \sin\varphi \int_0^{\pi} \frac{1-\cos t}{[\sqrt{1+\cos 2\varphi \cos t}]^3}\,dt - \frac{1}{\sin\varphi} I_z \\ I_o &= \cos 2\varphi I_m I_n - (a-1)(I_m \sin\varphi - I_n) I_s. \end{aligned}\right\} \tag{39}$$

At the bifurcation point, $I_o = 0$ holds, i.e.

$$a = 1 + \frac{\cos 2\varphi I_m I_n}{I_s[\sin\varphi I_m - I_n]}. \tag{40}$$

Figure 6 shows the relation of a and this bifurcation point $\xi = \xi_2$. This bifurcation point is the transitional point of the deformation from the torsional mode to the bending mode. So the larger the flexural rigidity is as against the torsional rigidity, the larger ξ_2 is. But ξ_2 never exceeds 0.698 for any value of a. This point is the bifurcation point under $(\kappa_3)^* = 0$. The bifurcation occurs for the arbitrary value of a, which is different from the case $\phi_m = 0$.

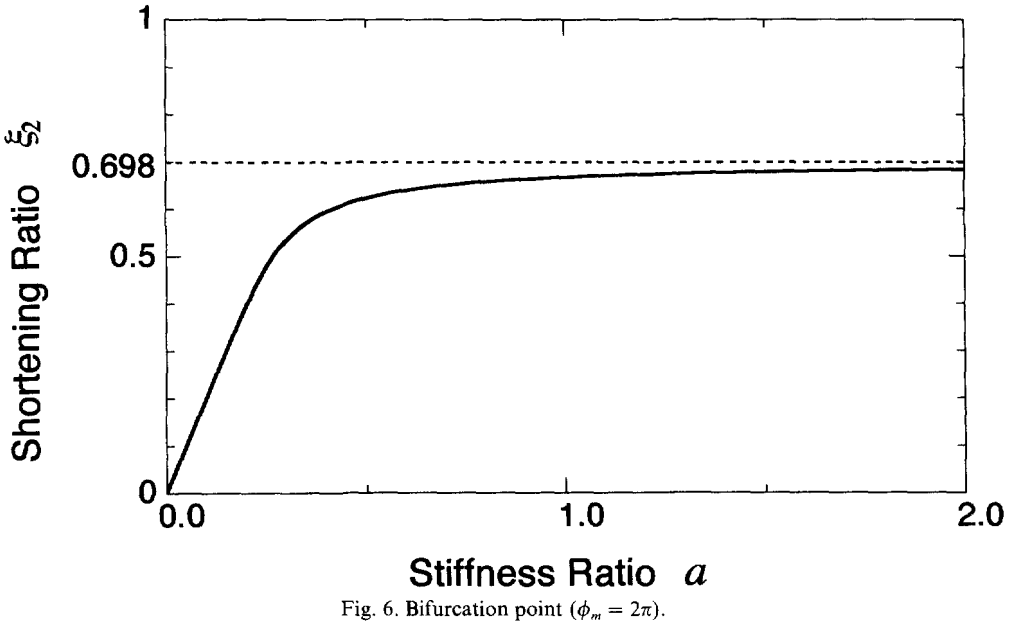

Fig. 6. Bifurcation point ($\phi_m = 2\pi$).

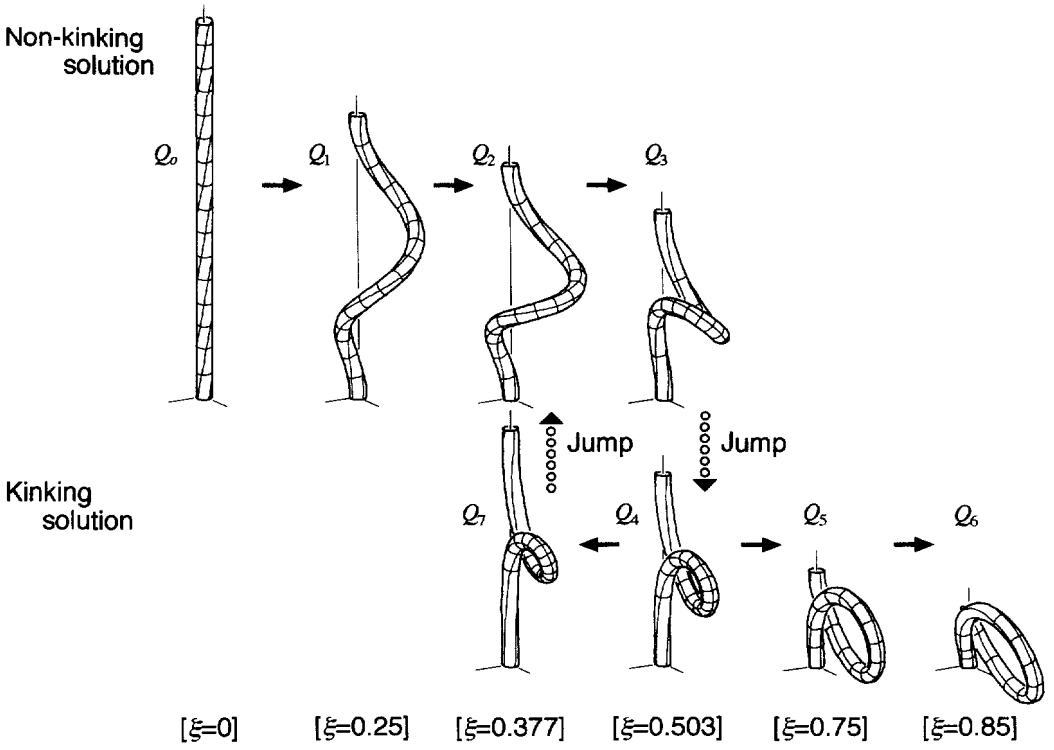

Fig. 7. Deformed shapes ($\phi_m = 3\pi$).

Figure 7 shows the deformed shapes of the elastica under $\phi_m = 3\pi$. Figure 8 plots the terminal thrust $T = P_3(0, \tau)$ and the total strain energy Π as a function of ξ, respectively. T and Π are normalized by the Euler buckling load $P_{cr} = -A\pi^2/l^2$ and $\Pi_o = A\pi^2/2l$, respectively. As seen in these figures, the non-contact solution does not exist when ξ exceeds the critical value $\xi_{cr} = 0.507$. There exist two non-contact solutions when $\phi_m > 2\pi$ and $\xi < \xi_{cr}$. One is the semi-kinking solution and the other the non-kinking one. Each solution coincides with the other at the critical point $\xi = \xi_{cr}$. The contact solution exists for $\xi \geqslant 0.377$. We call it the kinking solution hereinafter. Let us consider the deformation process of the elastica on Figs 7 and 8. After the elastica buckles at $\xi = 0$, it deforms along the non-kinking path ($Q_o \rightarrow Q_3$). At the critical point Q_3, it suddenly jumps into the kinking state Q_4. After that, it deforms along the kinking path for the subsequent end-extension ($Q_4 \rightarrow Q_7$) as well as the end-shortening ($Q_4 \rightarrow Q_6$). The contact results in the decrease of

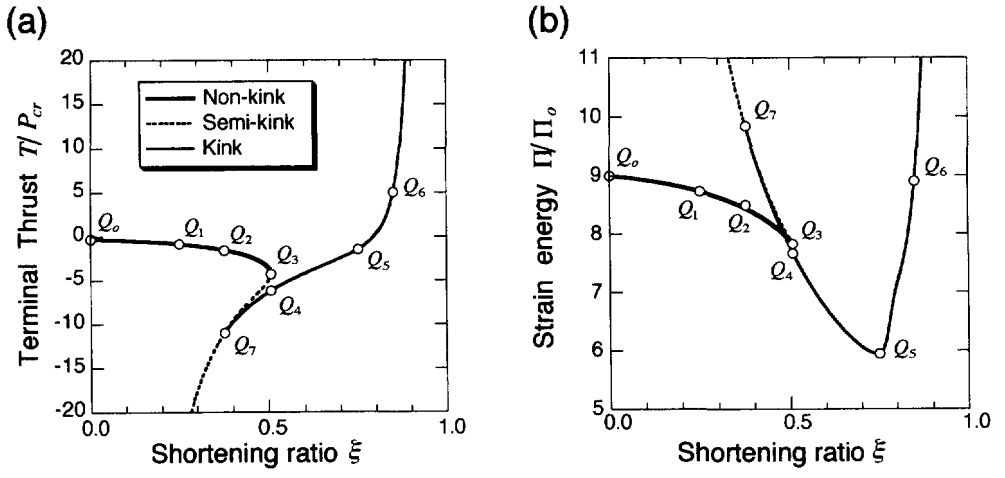

Fig. 8. Twist-shortening process under $\phi_m = 3\pi$ (a) terminal thrust $T(P_{cr} = -A\pi^2/l^2)$ (b) total strain energy $\Pi(\Pi_o = A\pi^2/2l)$.

the terminal tension and the total strain energy. For the subsequent end-extension, the terminal tension increases and the kinking tightens. For the large end-shortening, the terminal thrust transits from tensile to compressible force and goes off to infinity because of the constraint induced by the contact. When the elastica is terminally extended along the kinking path, the contact force decreases and vanishes at $\xi = 0.377$ (Q_7), where the kinking state coincides with the semi-kinking state. For $\xi < 0.377$, the contact force of the kinking elastica is negative and the semi-kinking elastica intersects itself. These solutions are thereby physically meaningless, and we can conclude that the elastica jumps back into the non-kinking state at $\xi = 0.377$. Thus the elastica cannot deform along the semi-kinking path. Figure 8 shows that T/P_{cr} decreases for the end-shortening along the non-kinking path, where the solution is unstable for axial compression if the end of the elastica is load-controlled. Other calculations show that the non-kinking solution is unstable at the buckling point $\xi = 0$ for $\phi_m \geqslant 1.69\pi$ although the buckling load is compressive for $\phi_m < 2.83\pi$.

The critical value ξ_{cr} gets smaller when ϕ_m gets larger as a gets larger (Fig. 9). Roughly speaking, the elastica reaches the critical state more easily for the smaller flexural rigidity compared with the torsional rigidity. Figure 10 shows the distribution of the bending energy (π_b) and torsional energy (π_t) along the arc length of the elastica at $(\xi, \phi_m) = (0.4, 3\pi)$. Each energy is normalized by $\pi_o = A\pi^2/2l^2$. In the semi-kinking and kinking cases, the bending energies concentrate extremely about $s = l/2$, and the torsional energies are much less than the bending energies. From these figures, we can conclude that the jump from the non-kinking to the kinking state is the transition of the torsional energy to the bending energy.

5.2.2. *Comparison with "the shortening-twist problem".* It is well known that the solution depends on the order of the application of load or displacement in a certain boundary value problem (e.g., Griner, 1984). Such a phenomenon is also observed in our problems. In the shortening-twist problem, there are additional solutions which do not appear in the twist-shortening problem.

As discussed in the previous section, three dimensional deformation occurs with no terminal twist for $\xi > 0.667$ with $a = 1$. Figure 11(a) shows the deformed shapes in the twisting process $\xi = 0.75$, and the corresponding value of the terminal torsional moment $M_t = M_3(0, \tau)$ is shown in Fig. 12(b). There are three solutions (S_1, S_3, S_5) for $\phi_m = 0$, which are related to others in the twisting process such as in Fig. 11(b). In Fig. 11(b), the solution curves represented in bold lines appear also in the twist-shortening process while those represented in broken lines never appear. Figure 12 illustrates the torsional moment M_t as the function of the shortening ratio ξ and the twist angle ϕ_m. This figure clearly shows that

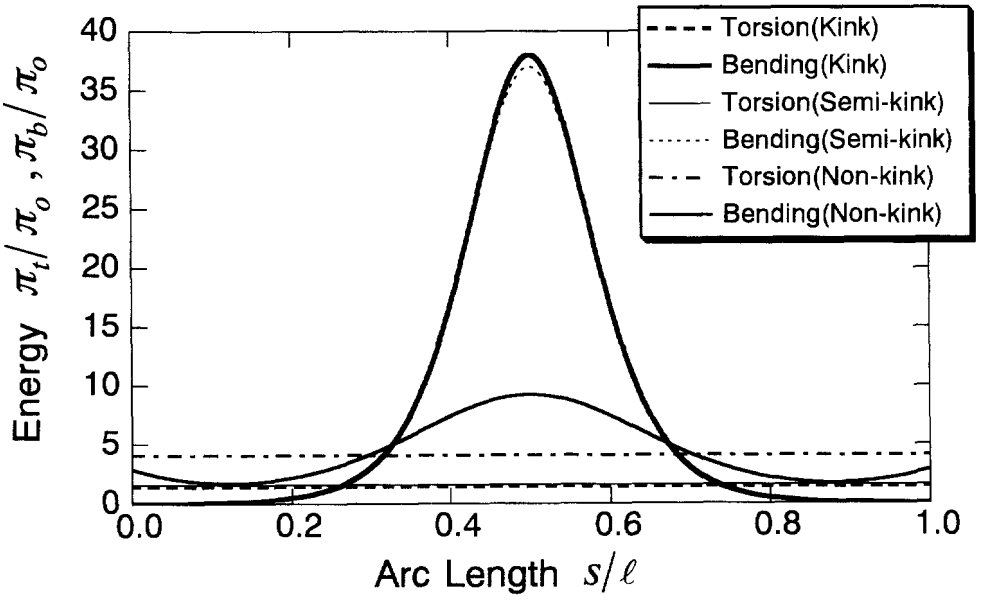

Fig. 9. Distribution of strain energies $\pi(\pi_o = A\pi^2/2l^2)[(\xi, \phi_m) = (0.4, 3\pi)]$.

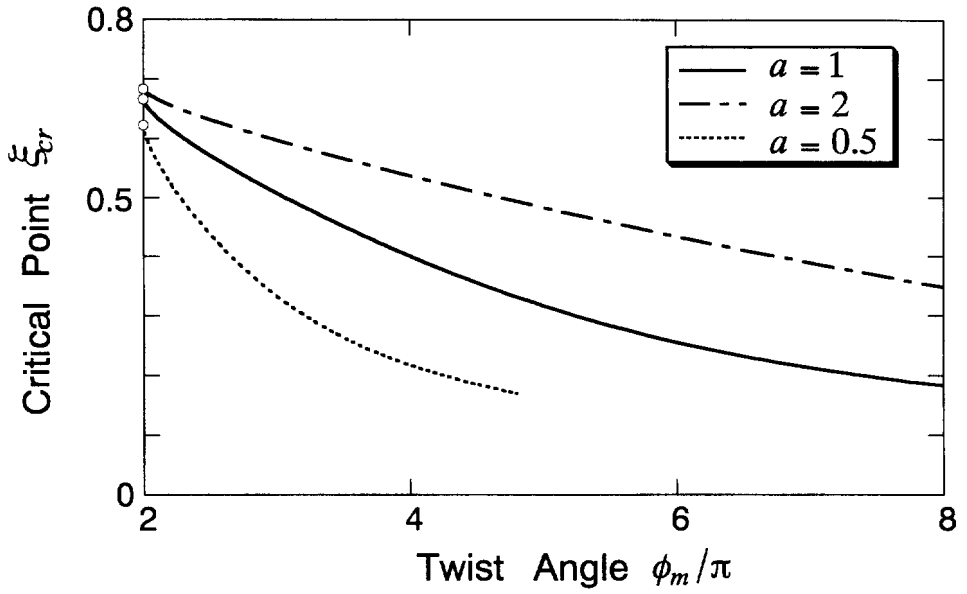

Fig. 10. Critical point of kinking.

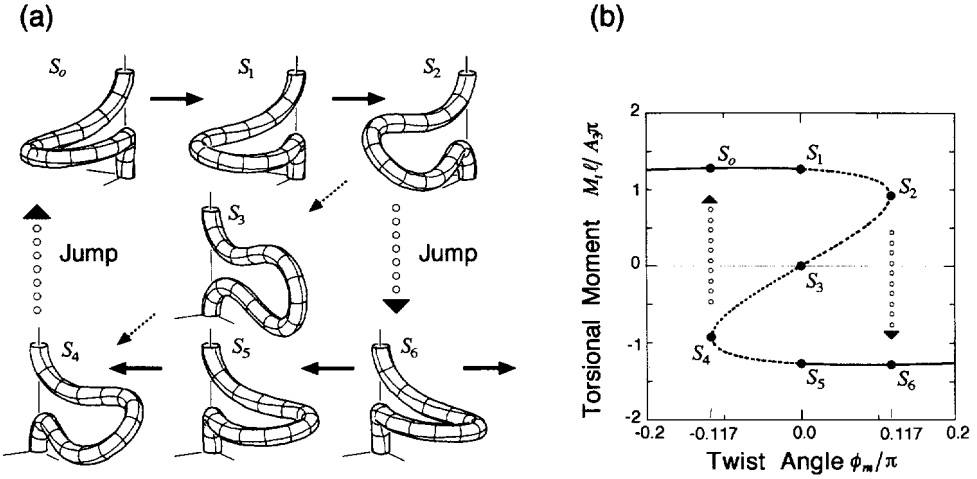

Fig. 11. Shortening-twist process under $\xi = 0.75$ (a) deformed shapes (b) torsional moment.

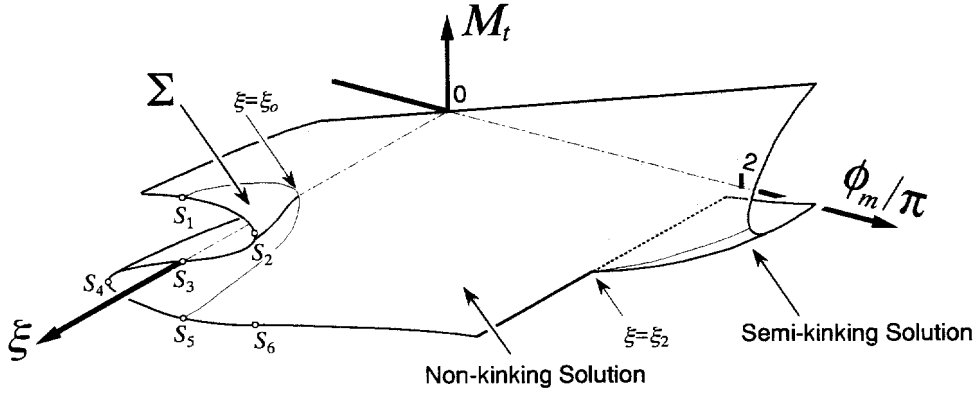

Fig. 12. Torsional moment M_t.

the deformation represented by the solution surface Σ never occurs in the twist-shortening process. We can also see from Fig. 11(b) that the snap-through phenomenon occurs from S_2 to S_6 in the increasing process of ϕ_m ($S_1 \rightarrow S_2$).

5.3. *Extensible elastica*

There are three main differences between the present elastica model and the Kirchhoff model: (1) there exists a "trivial" solution in the present model. This solution corresponds to the pre-buckled elastica which is uniformly twisted of the angle ϕ_m and uniformly compressed of the strain $\gamma_3 = -\xi$. The non-kinking solution should be regarded as the bifurcated solution from the trivial one. (2) The buckling does not occur at $\xi = 0$ in general. The buckling occurs at $\xi > 0$ if the buckling load is the compressive force, while at $\xi < 0$ if the force is tensile. In the latter case, the elastica buckles into the non-kinking state only with the terminal twist and no end-shortening. (3) There exists no kinking or semi-kinking solution at $\xi = 0$ in case of the Kirchhoff model because the elastica is assumed to yield no extension. The present model includes the effect of extension and we can analyze the kinking elastica at $\xi = 0$.

Let us fix our attention to the special behavior of the elastica at $\xi = 0$. Figure 13(a) and (b) respectively shows the change of the deformed shape and the applied torsional moment under $\xi = 0$ in the case $(a, p, q, d/l) = (0.5, 0, 0.2, 0.02)$. In the way of the twisting process, the elastica buckles from the trivial state into the non-kinking state at $\phi_m = 1.43\pi$ (D_1). For the subsequent twist, the elastica deforms along the non-kinking path ($D_1 \rightarrow D_4$), and forms a kink at $\phi_m = 2.29\pi$ ($D_4 \rightarrow D_5$). In the decreasing process of the terminal twist, the elastica jumps back into the non-kinking state at $\phi_m = 2.05\pi$ ($D_5 \rightarrow D_3$). Thus hysteresis exists in $2.05\pi < \phi_m < 2.29\pi$.

It must be noted that the effect of the transverse shear is not significant in "twist-shortening problem" compared with that of the extension. We can obtain rough estimation of the transverse shear effect from eqn (19). The effect of shear flexibility p appears mainly in the z-coordinate, i.e., the position component in the direction of the terminal force. Thereby it may be concluded that the transverse shear gives some effect on the value of the shortening ratio when some special phenomenon such as the kinking appears. Figure 14 shows the relation between p, q, and the critical value ξ_{cr} of the kinking under

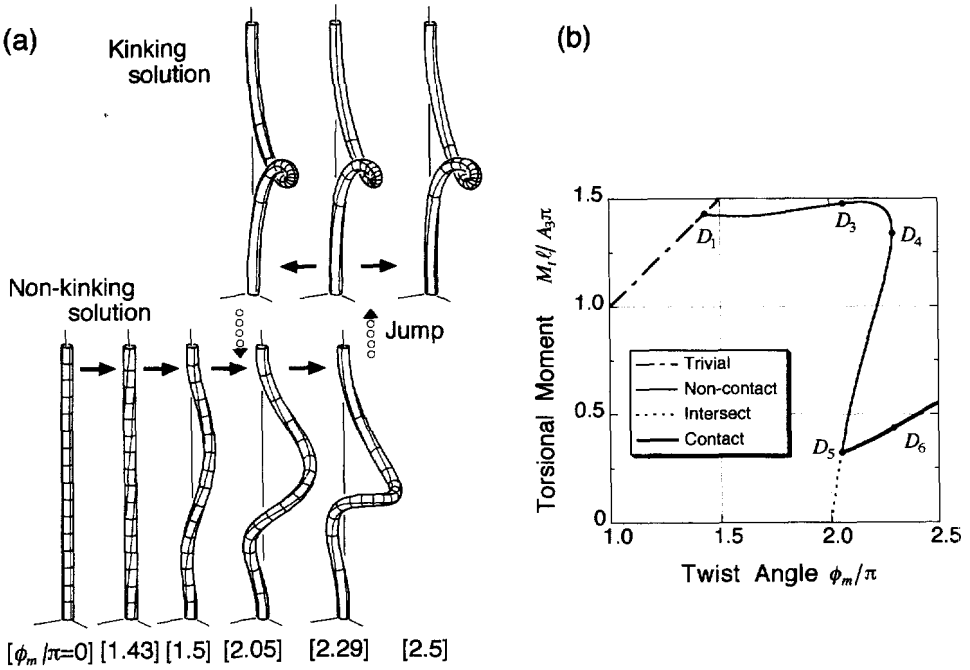

Fig. 13. Twisting process under $\xi = 0$[$a = 0.5$] (a) deformed shapes (b) torsional moment.

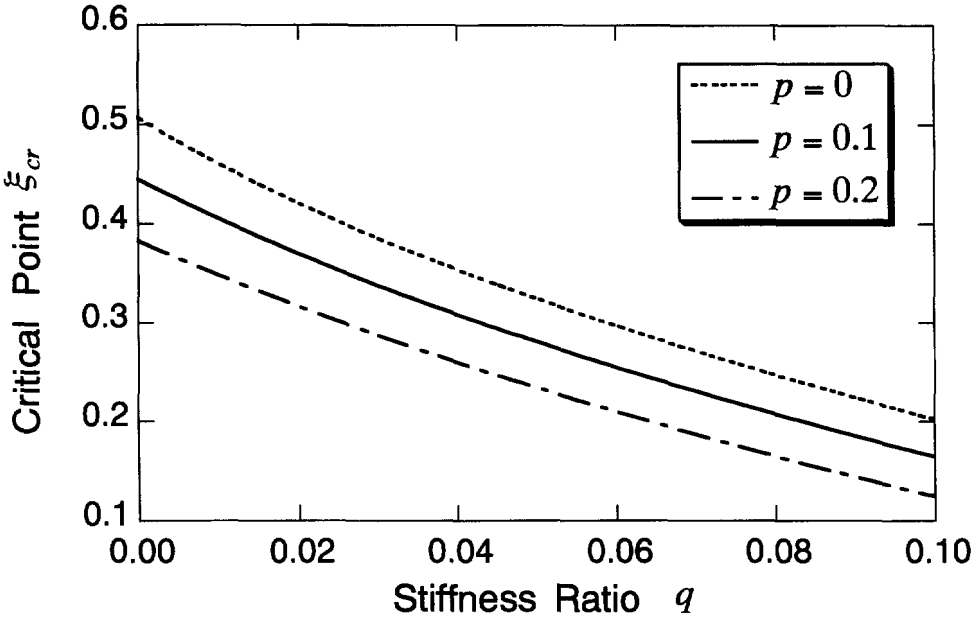

Fig. 14. Effect of transverse shear and extension on the critical point of kinking.

$(a, \phi_m) = (1, 3\pi)$. The larger shear flexibility as well as the larger extension flexibility causes the smaller critical value.

6. CONCLUDING REMARKS

A closed-form solution is derived for extensible, shear-flexible spatial elastica with equal principal stiffness under the assumption of no distributed load. The problem of the polar singularity inherently associated with the Euler angles is clearly resolved.

To demonstrate the validity and the applicability of the present solution, two boundary value problems are considered, i.e., "the twist-shortening problem" and "the shortening-twist problem". The contact problem is solved in the case where the elastica contacts with itself and forms a kink. From the theoretical observation and the numerical analysis, the global qualitative and quantitative behaviors of a spatially buckled elastica are clarified, and the theoretical explanation is given to the well-known phenomena, e.g., the secondary buckling, snap-through behavior, catastrophic formation of a kink.

In this paper, four assumptions are used with respect to the constitutive relations and the external force (see Section 2). Many researchers study more general cases with fewer assumptions by both theoretical and numerical approaches. The authors hope the present results may be available for other studies.

Acknowledgments—The authors would like to thank Prof. Miura, Prof. Onoda (Institute of Space and Astronautical Science Japan), Prof. Hisada, Dr. Watanabe (University of Tokyo), and Dr Noguchi (Keio University) for their helpful discussions. The authors also thank the editors for introducing very important references [Rosenthal (1976), Maddocks (1984)].

REFERENCES

Antman, S. S. (1974). Kirchhoff problem for nonlinearly elastic rods, *Quarterly Applied Mathematics* **32**, 221–240.

Antman, S. S. and Kenney, C. S. (1981). Large buckled states of nonlinearly elastic rods under torsion, thrust, and gravity. *Archives of Rational Mechanical Analysis* **76**, 289–338.

Buzano, E., Geymonat, G. and Poston, T. (1985). Post-buckling behavior of a non-linearly hyperelastic thin rod with cross-section invariant under the dihedral group D_m. *Archives Rational Mechanical Analysis* **89**, 307–388.

Felippa, C. A. and Crivelli, L. A. (1991). A congruetial formulation of nonlinear finite elements. In *Nonlinear Computed Mechanics* (eds Wriggers, P. and Wagner, W.). Springer-Verlag, Berlin, pp. 283–302.

Goto, Y., Yoshimitsu, T. and Obata, M. (1990). Elliptic integral solutions of plane elastica with axial and shear deformations. *International Journal of Solids and Structures* **26**, 375–390.

Griner, G. M. (1984). A parametric solution to the elastic pole-vaulting pole problems. *ASME Journal of Applied Mechanics* **51,** 409–414.

Huddleston, J. V. (1978). The compressible elastica in three dimensions. *International Journal of Mechanical Sciences* **20,** 229–236.

Iura, M. and Atluri, S. (1988). Dynamics of highly-flexible space-beams undergoing large overall motions. *AIAA*-88-2413, *AIAA/ASME/ASCE/AHS 29th Structures, Structural Dynamics and Materials Conference*, Williamsburg, 18–20 April.

Kovari, K. (1969). Raumiliche verzweigunsprobleme des dunnen elastischen stabes mit endlischen verformungen. *Ingenieur-Archiv* **37,** 393–416.

Love, A. E. H. (1952). *The Mathematical Theory of Elasticity*. Cambridge University Press, Cambridge, pp. 256–280.

Maddocks, J. H. (1984). Stability of nonlinear elastic rods. *Archives of Rational Mechanical Analysis* **85,** 311–354.

Nordgren, R. P. (1974). On computation of the motion of elastic rods. *ASME Journal of Applied Mechanics* **41,** 777–780.

Nour-Omid, B. and Rankin, C. C. (1991). Finite rotation analysis and consistent linearization using projectors. *Computer Methods of Applied Mechanical Engineering* **93,** 353–384.

Reissner, E. (1981). On the finite deformations of space-curved beams. *Journal of Applied Mathematical Physics (ZAMP)* **32,** 734–744.

Rosenthal, F. (1976). The application of Greenhill's formula to cable hockling. *ASME Journal of Applied Mechanics* **43,** 681–683.

Ross, A. L. (1977). Cable kinking analysis and prevention. *ASME Journal of Engineering for Industry* **99,** 112–115.

Watanabe, H., Hisada, T. and Noguchi, H. (1992). Kinking analysis of rubber band by hyperelastic finite element method. In *Proceedings of the Symposium on Space Structures*, Sagamihara, 3–4 December, pp. 185–191.

Yabuta, T., Yoshizawa, N. and Kojima, N. (1982). Cable kink analysis: cable loop stability under tension. *ASME Journal of Mechanics* **49,** 584–588.